Chemometrics and Intelligent Laboratory Systems 234 (2023) 104761

Contents lists available at ScienceDirect

Chemometrics and Intelligent Laboratory Systems

journal homepage: www.elsevier.com/locate/chemometrics

Fast characterization of in-plane fiber orientation at the surface of paper sheets through image analysis

Paulo A.N. Dias [a], Ricardo J. Rodrigues [b], Marco S. Reis [a,*]

[a] University of Coimbra, CIEPQPF, Department of Chemical Engineering, Rua Sílvio Lima, 3030-790, Coimbra, Portugal
[b] RAIZ – Forest and Paper Research Institute, Quinta de São Francisco, Rua José Estevão (EN 230-1), 3800-783, Eixo, Aveiro, Portugal

ARTICLE INFO

Keywords:
Papermaking
In-plane fiber orientation distribution
Measurement of fiber orientation angle and anisotropy
Image analysis
Reflective based imaging

ABSTRACT

The in-plane fiber orientation distribution has a decisive impact on paper mechanical and dimensional properties (e.g., tensile stiffness, hygroexpansion). It is usually estimated offline through relatively expensive bench instrumentation such as diffusion-based optical methods and ultrasonic devices. In this work we present an alternative methodology that is fast, portable, inexpensive and able to provide the complete surface polar fiber orientation profile. The proposed technology combines an image acquisition setup, consisting of a digital camera with a low angle illumination system, with the gradient-segmentation method (GSM), a robust image analysis algorithm. This camera-GSM methodology presented high internal consistency, accurately identifying the angles of samples subjected to known rotations at the imaging step. The methodology also produced comparable results to the TSO (tensile stiffness orientation) technique, used as reference. The methodology is easily transferable to plant operation, including for the online assessment of fiber orientation.

1. Introduction

Pulp fibers are flexible and collapsible materials with varying lengths and shapes [1,2]. As a consequence, they assume irregular configurations when forming a paper sheet, that can be represented by the polar fiber orientation distribution function [3]. Two parameters are usually extracted to summarize the entire distribution function for the purposes of assessing its impact on paper properties (see Fig. 1): i) orientation angle, θ_{max}, corresponding to the angle between the major direction of the paper sheet (also known as the machine direction, MD, i.e., the direction parallel to the paper machine where the paper is produced) and the direction with the highest orientation level; ii) anisotropy, A, obtained by the ratio of the maximum, a, and minimum, b, values of the fiber orientation distribution function, $A = a/b$ [3,4]. In a paper machine, fibers are predominantly aligned in MD when compared to the cross-machine direction (CD, which is the direction perpendicular to MD) [5,6]. This anisotropic fiber distribution has a significant impact on critical paper properties for the end user, such as the paper tensile stiffness index (TSI), tensile index, drying shrinkage, wet straining, hygroexpansion and curl tendency [7–10]. Therefore, the proper measurement of fiber orientation distribution is of vital importance for the paper industry, to ensure compliance with quality specifications, as well as for R&D activities, namely to understand and predict the paper behavior for different levels of fiber orientation.

Methodologies used to analyze fiber orientation can be organized into two groups [11,12]: i) direct approaches, that require the preliminary characterization of the orientation of individual fibers; ii) indirect methods, in which the estimated polar distribution is obtained by adopting measurement principles that correlate with the underlying distribution of individual fibers. These methodologies are typically applied for offline measurement.

1.1. Direct methods for measuring fiber orientation

Methods from this group extract information directly from fibers disposed on a paper sheet. In a typical direct method, a small quantity of the pulp is previously stained before the papermaking process, allowing the orientation of the stained fibers to be determined by image analysis approaches [11–13]. However, the irregular configurations assumed by the flexible and overlapping fibers in the paper structure [3] raises several difficulties for an image analysis methodology to accurately estimate their orientation [11]. A recently developed method addresses these challenges, by combining a sheet splitting method, a layer imaging approach with a flatbed scanner and an image analysis methodology to determine the orientation of all the fibers of a previously dyed sample.

* Corresponding author.
E-mail address: marco@eq.uc.pt (M.S. Reis).

https://doi.org/10.1016/j.chemolab.2023.104761
Received 2 September 2022; Received in revised form 13 November 2022; Accepted 15 January 2023
Available online 18 January 2023

Nomenclature

a	maximum of the fiber orientation distribution function
A	anisotropy, obtained by the ratio of the maximum, a, and minimum, b, values of the fiber orientation distribution function
b	minimum of the fiber orientation distribution function
CD	cross-machine direction, i.e., the direction perpendicular to MD
$f_I(x,y)$	intensity function for a pixel at a position (x,y) in the digital image
$f_\theta(\theta)$	cosine function with three terms, a Fourier series expansion truncated in the third term, used to represent the fiber orientation distribution
h_x	convolution mask of the Sobel operator for the direction x of the digital image
h_y	convolution mask of the Sobel operator for the direction y of the digital image
K	scale factor of cosine function with three terms
MD	machine direction, i.e., the direction parallel to the paper machine where the paper is produced
n	number of rotations tested, i.e., number of θ_{off} introduced at an imaging step for the internal consistency assessment
p-tile	percentage of pixels in the images probably belonging to fiber segment edges, of higher gradient magnitude
r_1	first parameter of the linear regression of θ_{max} as a function of θ_{off}
r_2	second parameter of the linear regression of θ_{max} as a function of θ_{off}
R^2	coefficient of determination
$\overline{\lvert RD \rvert}$	average of the modulus (absolute value) of relative deviation, $\lvert RD \rvert_i$, for all the n considered offset angle points i, introduced at an imaging step for the internal consistency assessment
$\lvert RD \rvert_i$	absolute value of the relative deviation of the anisotropy at a given offset angle with index i, A_i, from the standard measurement ($\theta_{off} = 0°$), $A(0°)$
TSI	tensile stiffness index, N m/kg
x	horizontal axis of the digital image
y	vertical axis of the digital image
ZD	thickness direction of a paper sheet

Greek letters

$\nabla f_I(x,y)$	gradient of the intensity function $f_I(x,y)$ of a pixel at position (x,y)
$\lvert\nabla f_I(x,y)\rvert$	magnitude of the gradient of the intensity function $f_I(x,y)$ of a pixel at position (x,y)
η_1	first term of the cosine function with three terms
η_2	second term of the cosine function with three terms
η_3	third term of the cosine function with three terms
θ	orientation angle of a fiber segment, corresponding to the angle between MD and the longitudinal direction of the fiber segment
θ_{off}	offset angle, corresponding to a rotation relative to MD introduced at an imaging step
θ_{max}	orientation angle, corresponding to the angle between MD and the direction with the highest orientation level of fibers, °
σ_{avg}	standard deviation of the mean, estimated from the sample standard deviation of the n data points, $\hat{\sigma}$, using $\sigma_{avg} = \frac{\hat{\sigma}}{\sqrt{n}}$
φ	angle (direction) of the gradient of the intensity function $f_I(x,y)$ of a pixel at position (x,y)

Subscripts

i	offset angle (θ_{off}) point

Acronyms

dpi	dots per inch
GSM	gradient-segmentation method
RGB	red, green and blue color space
TSO	tensile stiffness orientation, measurement equipment
WGM	weighted gradient method

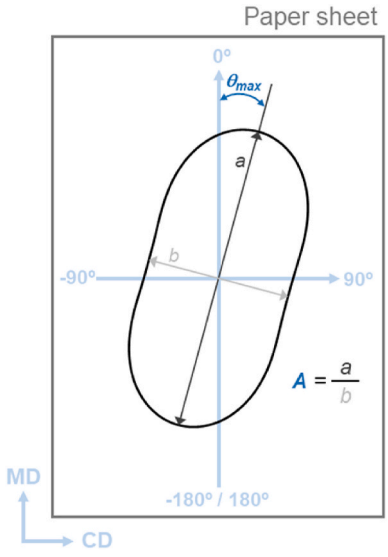

Fig. 1. Exemplification of the in-plane surface polar fiber orientation distribution in a paper sheet. The visual definition of the orientation angle, θ_{max}, and of the anisotropy, A, is shown.

For an 80 g/m^2 sheet sample, the method requires obtaining 60 to 100 layers to effectively separate the individual fibers. A segmentation method is then used to detect the fibers, followed by a skeletonization technique to find the fiber center lines. Segments are obtained by dividing the previously found fiber center lines, with the orientation of these segments being subsequently determined [14,15]. Although providing repeatable and accurate results, this direct methodology is expensive, highly time consuming and requiring advanced training to be executed [14], limiting its practical application [11,14].

1.2. Indirect methods for measuring fiber orientation

Indirect methods to estimate fiber orientation are easier to apply, being typically adopted in practice [11]. Currently adopted methodologies include the analysis of x-ray diffraction, microwave dielectric anisotropy, mechanical properties, optical techniques and β-radiography [3,11,16]. X-ray diffraction was proposed to estimate fiber orientation distribution by analyzing the scatter pattern of an incident X-ray beam [11]. The method assumes the cellulose chains to be predominantly oriented along the fiber axis [3], allowing results to correlate well with fiber orientation [11]. The microwave methodology is based on the measurement of the sheet dielectric anisotropy, presenting limitations regarding the dependence to the sheet moisture content [17].

Mechanical properties such as tensile strength or stiffness based parameters depend strongly on the fiber orientation distribution. The

latter parameters are usually applied, being determined by tensile mechanical testing or by ultrasonic method [11,18–20]. The elastic modulus, a stiffness based parameter, requires the knowledge of the paper thickness, a property difficult to measure. For that reason, it is preferable to use the tensile stiffness index (TSI), a property independent of the thickness [18]. Unlike the tensile testing technique, the ultrasonic method is non-destructive, and able to provide the in-plane TSI distribution by measuring the velocity of the ultrasound through the sheet at different angles [18,20–22]. Although being widely applied in the paper industry [12,13,23,24], the ultrasonic methodology is highly dependent of internal stresses introduced by wet pressing and applied drying restrictions [12,13,19–21,24]. Therefore, the measured TSI distribution may deviate from the actual fiber orientation, conditioning the analysis of the results in certain circumstances [12,19,20,24].

Contrary to the ultrasonic method, optical techniques are not influenced by the sheet internal stresses [3,11,13,23,24]. Optical methods are based on the analysis of patterns resulting from light diffraction and diffusion, and on the analysis of images obtained from light reflection or transmission [3,11,16]. For the light diffraction methods, light is diffracted by individual fibers forming a pattern with higher intensity perpendicularly to the direction of maximum fiber orientation [11,25,26]. However, these methods are less attractive, being highly dependent on the sheet basis weight [26]. A typical diffusion method analyzes the diffused light resulting from the interaction of an incident laser beam with the fibers. Several detectors are used to identify the diffused light, with an intensity pattern being formed that correlates with the fiber distribution of the sample [11,23,24,27].

A recently developed system illuminates a paper sample region with two laser beams, one at a time. Each laser is directed perpendicularly to one of the sheet surfaces, bottom and top. A detector is placed above each one of the two surfaces, capturing images with the patterns of the transmitted and of the retro-diffused light, respectively, obtained due to the interaction of one of the lasers with the sample. The patterns in the captured images are then analyzed to obtain the orientation angle and the anisotropy [4,28]. Although providing reliable results [4,11,23,24,28] and offering online measurement capability to monitor in real time the fiber orientation in the two faces of the produced paper [27], the diffusion methods are complex, requiring the use of relatively expensive hardware (at least, when compared to a digital camera based technique). Alternatively, methodologies combining imaging techniques (usually optical methods) with image analysis can also be applied.

Confocal laser scanning microscopy was used to obtain digital images for previously dyed samples. With this method, images for several depths can be acquired, allowing the study of the variation of fiber orientation distribution over the thickness direction (ZD) of paper [29]. In Ref. [16], images of paper samples obtained through optical light transmission and β-radiography are analyzed.

Digital images of reflected light from sample surfaces can also be obtained by an optical microscope [3,30], a digital camera [31,32] and a flatbed scanner [5,6]. These imaging systems can be complemented by using a dark background, to increase the contrast of fibers in thin layers/papers [5,6,31], and/or a low angle illumination system, to improve the visualization of existing structures in the paper surface [30,32]. The use of a digital camera is particularly interesting, allowing the development of online measurement solutions for the paper machine [32].

1.3. Image processing algorithms

Image analysis-based strategies are widely applied in the industry [33–35]. These approaches are also very relevant for the paper sector, being used for several applications such as the online assessment of the paper surface quality and the characterization of relevant structural features [35,36]. Among the structural features, the characterization of the fiber orientation has been the focus of several research works. Next, the most relevant image and signal processing algorithms proposed in the literature to characterize the fiber orientation are briefly presented and discussed.

Previous works suggested the analysis of acquired images using Fourier transform based approaches. The obtained greyscale digital images are previously subjected to a binarization operation through a simple moving average method and dynamic thresholding [3,29,30]. Although this preprocessing operation reduces the computational burden, the application of the Fourier transform remains a time-consuming procedure [3]. Nevertheless, this perceived disadvantage is becoming less relevant due to the increasing availability of computational power. A method was also proposed to estimate fiber orientation distribution [37] of blurred greyscale images of paper layers obtained by a delamination method [31]. Lines with uniform length are drawn for several directions in the image, with the variation of grey level resulting in scaled variograms along each line. The orientation distribution is then obtained by numerical treatment [37]. Previous works also suggested the application of Hough transform [38,39], a segmentation based image analysis method that allows the detection of borders [40]. Although being widely applied as an image analysis tool, the Hough transform is considered by some authors to be computationally highly demanding [40], a fact that can be mitigated given the current access to affordable computational power. A more recent work suggested the use of the steerable filtering method to estimate the fiber orientation distribution. Despite being less sensitive to noise in the image, the steerable filtering method is more complex to run and implement, consuming more computational resources to provide results in a timely manner [41].

An alternative methodology applied the concept of local gradient functions of grey level images. For each pixel, a gradient vector of the intensity is obtained, which is characterized by two parameters: the corresponding magnitude and direction angle. The local dominant orientation and anisotropy is then calculated by applying texture analysis procedures [16,42–44]. An higher contrast between fibers is attained in paper layers obtained by delamination when compared to unprocessed paper surfaces, allowing for the application of a version of the method of the gradients to reflective based images with lower resolutions, of around 800 dpi (dots per inch) [31,45]. The magnitude of the local gradient is used as an indicator of the probability of the corresponding pixel being part of a fiber edge. Consequently, the magnitude is typically used as a weighting factor for the contribution of each pixel to a weighted probability density function of local orientations [45,46]. Alternatively, a thresholding approach can also be applied to the magnitude of the gradient. In this case, the density function of local orientations is determined by considering equal contributions from the pixels with values of the magnitude of the gradient above the selected threshold, which are considered as being part of a fiber segment edge. However, the criterion used to define the threshold is not presented by the authors [5,6,41]. Once the density function of local orientations is obtained, the anisotropy and the orientation angle are then computed [5,6,31,41]. This type of approach is more efficient, requiring low computational effort when compared to other image analysis based techniques [14,41]. However, the application of this type of method to paper surfaces requires an improved reflective based imaging system and/or images of increased resolutions [32].

1.4. Objectives and organization

Analyzing the methodologies presented above, one can observe that they often require moderately expensive equipment and time consuming protocols. In image-based methods, the algorithmic approach may also be computationally demanding for online use. This is an important factor as more and more monitoring methods are not implemented in a centralized way on main servers and DCS, but locally in distributed computing environments (e.g., through edge computing) where computational power and memory are still limiting factors (e.g., for reasons related to energy consumption and limited bandwidth). As such,

the algorithmic approach should be carefully assessed regarding its final accuracy and implementation complexity. The goal of this work is to develop a fast, portable, inexpensive, and accurate technology to determine the in-plane surface polar fiber orientation distribution of uncoated paper sheets. The methodology combines a reflective based imaging system to obtain digital images with a fast and robust gradient-based image analysis technique to identify the fiber edges. The imaging system consists of a digital camera coupled to a low angle illumination system. This work is important for R&D and quality control laboratorial applications to guarantee fast, reliable and affordable fiber orientation measurements, offline, avoiding the use of costly techniques such as diffusion based optical methods and ultrasonic measurements. Moreover, the technology developed has potential for effective online industrial application, to enable quality measurements of fiber orientation in real time and at low cost, following the trend of increasing digitalization of Industry 4.0 [47].

This article is organized as follows. In Section 2, the methodology developed to estimate in-plane surface fiber orientation distribution is presented. The procedure followed to validate the methodology is also described, including the production of laboratory paper sheets of different levels of fiber anisotropy for testing. In Section 3, the main results obtained to test and validate the methodology are presented and discussed. Finally, the main conclusions are summarized, and some perspectives are shared on future work.

2. Materials and methods

The proposed methodology was tested on laboratory sheets produced in a dynamic former. In this section we describe how the test sheets were prepared in the laboratory and present in detail the two steps of the proposed methodology: i) image acquisition – to collect digital images of sheet surfaces; ii) image processing – to obtain an estimate of the polar distribution of fiber orientation, as well as the main parameters of interest: orientation angle, θ_{max}, and anisotropy, A.

2.1. Sheet preparation

Laboratory anisotropic sheets were prepared from a suspension of refined industrial bleached *Eucalyptus Globulus* pulp fibers (PFI refiner set to 3000 rotations, Schopper-Riegler degree of 39°). Fibers typically have an average width of around 18.2 μm and a length of around 0.7 mm [48]. The suspension (2.0–2.5 g/l) was fed to a dynamic former to prepare three sheets (basis weight target of 80 g/m^2) with different levels of anisotropy: i) S1 (low level), jet pressure of 1.8 bar and wire speed of 900 m/min; ii) S2 (medium level), 1.5 bar and 1150 m/min; iii) S3 (high level), 1.5 bar and 1400 m/min. The formed sheets were subjected to three successive pressing steps of 200, 300 and 440 kPa in a laboratory rolling press, followed by a drying step, under full restriction, in a laboratory dryer at 50 °C for 30 min. The produced sheets were then kept in a room with controlled environment (temperature of 23 °C ± 1 °C, relative humidity of 50% ± 2%). The sample surfaces were identified by adding the letter B for bottom and T for Top, to the sheet acronym (e.g., S1B, bottom surface of S1).

The fiber orientation distribution of the prepared sheets was estimated by applying two methodologies: the method proposed in this work, that consists of a two-step procedure of image acquisition and image analysis, and an ultrasonic based method for comparison, using a tensile stiffness orientation (TSO) measurement equipment (TSO tester – Code 150, Lorentzen & Wettre, Sweden).

We would like to point out that the pressing procedure introduces some roughness two-sidedness in the laboratory sheets, with the bottom surface being clearly smoother (i.e., less roughness). To confirm this fact, the sheets were characterized with a Bendtsen equipment to determine the roughness of both surfaces. The roughness two-sidedness of the sheets does not impact the TSO measurements, which are based on the measurement of the propagation speed of ultrasonic pulses through the paper sheet [22]. However, it might affect the measurements performed by image analysis based methods, by decreasing the capability to observe individual fibers in the images from the bottom surface of the sheet when compared to the top. Therefore, the results obtained with the image analysis methodology for the two surfaces of a given sample, bottom and top, should not be compared directly. Instead, the results obtained for the samples should be compared for each surface: bottom – S1B, S2B e S3B; top – S1T, S2T e S3T.

2.2. Image acquisition

Digital images of the two paper surfaces, bottom and top, of sheet samples prepared by a dynamic former for three levels of anisotropy, were obtained by a digital camera coupled to a low angle illumination system using a dark background (Fig. 2). A digital camera (Manta G-125, Allied Vision, Germany) with an applied pixel resolution of 18 μm (corresponding to an image resolution of 1400 dpi) was used to capture RGB (red, green, blue) color images. The applied pixel resolution is within the typical width of the *Eucalyptus Globulus* fibers used in this work, and therefore is enough to allow the visualization of the fibers in the sample surface. Each image covers an area of the sample of around 23.4 × 17.5 mm^2 (CD × MD). Due to this small area, a total of 8 images were collected from different positions to accurately represent the entire sample surface. The anisotropy and orientation angle of each sample surface is obtained by averaging these quantities for the 8 collected images. The light exposure was set to 800 μs and the lens aperture was manually controlled and kept constant for all tests. An annular dark field illumination system (internal diameter of 82 mm and external of 117 mm) formed by a ring of LEDs (model DRL-V-R117/82H, Infaimon, Spain) was kept on top of the sample surface. The LEDs emit red light that forms a low angle with the paper surface (inferior to 30°). This low angle illumination system guarantees a symmetrical and uniform illumination of the sample from all the in-plane directions, allowing the surface structures to be highlighted and the reflections from highly reflecting parts to be eliminated [30].

2.3. Image analysis

The improved camera based imaging system proposed in Section 2.2 secures the acquisition of images of the paper surface with increased quality, allowing the use of efficient algorithms to estimate fiber orientation, such as those based on a gradient approach. In this context, a new gradient based algorithm was developed in this work. The proposed algorithm finds the dominant orientation of segment edges on a greyscale image by combining a gradient field approach, in which the changes in the intensities of pixels occurring at the edges of fiber segments and/or bundles are detected [31,40], with a segmentation

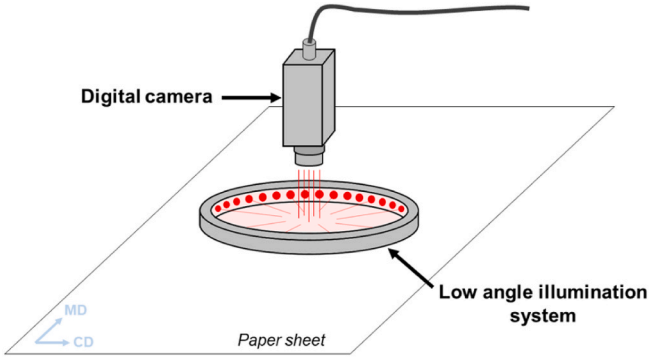

Fig. 2. Imaging apparatus combining a digital camera with a low angle illumination system based on a ring of LEDs emitting red light. (For interpretation of the references to color in this figure legend, the reader is referred to the Web version of this article.)

method, to determine the pixels that most likely regard to fiber segment edges [40,49]. The algorithm (see simplified flowchart in Fig. 3), designated in this work as the gradient-segmentation method (GSM), was implemented in Matlab (The Mathworks, Inc., U.S.A.) using custom-made code and built-in functions of the Image Processing Toolbox.

When required, a preliminary pretreatment phase is applied, where images are first transformed from the RGB color space to greyscale. It should be mentioned that a preliminary study (not presented here) showed that the type of image used, RGB or greyscale, does not impact the results obtained with the proposed algorithm. The specific sample surface under analysis also needs to be taken into account – the mirror image of bottom surfaces are obtained and studied, while top surface images are analyzed without further treatment.

After the pretreatment phase, the four main steps of the algorithm are implemented: (1) computation of the gradient of intensities of pixels; (2) setting the gradient magnitude threshold; (3) obtaining the frequency distribution for the angles of fiber segments; and (4) fitting a fiber orientation model to the frequency distribution data. Each step of the algorithm is described in detail next.

2.3.1. Computation of the gradient of intensities of pixels

Considering the horizontal (x) and vertical (y) axes of the digital image, the gradient of the intensity function $f_I(x,y)$ of a pixel at position (x,y) is a vector $\nabla f_I(x,y)$ with two components, magnitude, $|\nabla f_I(x,y)|$ in Eq. (1), and angle, φ in Eq. (2). In this work, angles are reported in degrees. To determine the components of the gradient vector, the first derivatives along the two natural geometric directions, $\frac{\delta f_I(x,y)}{\delta x}$ and $\frac{\delta f_I(x,y)}{\delta y}$, are first obtained [40].

$$|\nabla f_I(x,y)| = \sqrt{\left(\frac{\delta f_I(x,y)}{\delta x}\right)^2 + \left(\frac{\delta f_I(x,y)}{\delta y}\right)^2} \tag{1}$$

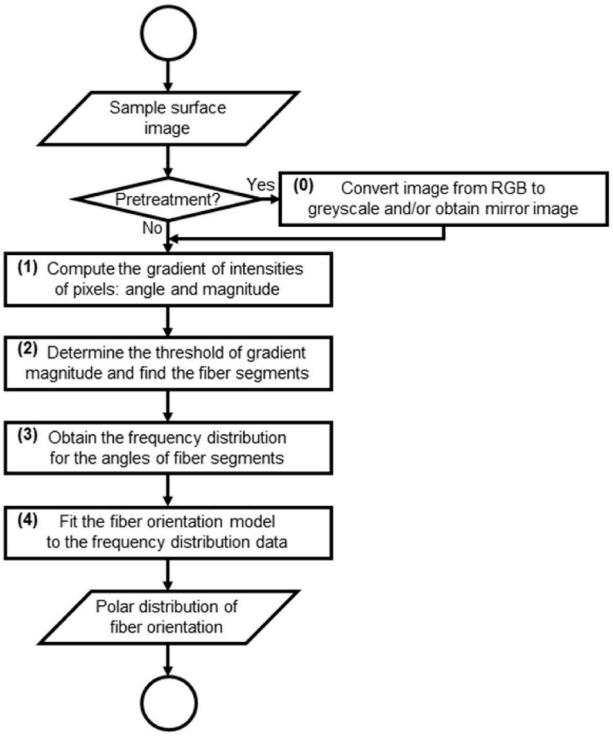

Fig. 3. Simplified flowchart of the gradient-segmentation method (GSM) developed in this work to determine the fiber orientation of the sample surface image.

$$\varphi = arctan\left(\frac{\frac{\delta f_I(x,y)}{\delta y}}{\frac{\delta f_I(x,y)}{\delta x}}\right) \tag{2}$$

Approximations of the first derivatives can be determined for each pixel by applying an appropriate convolution mask to the local neighborhoods. The estimates for each derivative are obtained by the weighted sum of the intensities of the pixels of the local neighborhood using the weights of the convolution mask. Estimates can also be obtained at the borders of the image. In these cases, the intensity of a neighborhood point that falls outside the image is estimated as being similar to the value of the closest image pixel. In this work, the Sobel operator was applied, consisting of two convolution masks represented by 3 × 3 matrices, h_x for direction x in Eq. (3), and h_y for direction y in Eq. (4); for more details see Ref. [40].

$$h_x = \begin{bmatrix} -1 & 0 & 1 \\ -2 & 0 & 2 \\ -1 & 0 & 1 \end{bmatrix} \tag{3}$$

$$h_y = \begin{bmatrix} 1 & 2 & 1 \\ 0 & 0 & 0 \\ -1 & -2 & -1 \end{bmatrix} \tag{4}$$

The gradient magnitude, $|\nabla f_I(x,y)|$, and the gradient angle, φ, are then determined by introducing the two convolution masks, h_x and h_y, in Eq. (1) and Eq. (2). As the gradient direction is orthogonal to the fiber segment direction, the final calculation of the fiber orientation angle, θ, is done by subtracting 90° to the gradient angle, φ [40].

2.3.2. Setting the gradient magnitude threshold

As mentioned before, pixels belonging to a fiber segment edge have higher gradient magnitudes. In this context, the image is composed by two sets of pixels: those that are part of fiber segment edges, with higher magnitudes, and those that are part of the background (includes the pixels that are within fiber segments and/or bundles), with lower magnitudes. Previous works have suggested the application of a threshold to the gradient magnitude, to determine which pixels belong to fiber segment edges. However, the methodology adopted to select such threshold was not referred by the authors. Nevertheless, the analysis of these works suggests that once the threshold is selected (by some unspecified way) it is kept constant for all the analyzed images [5,6,41]. In practice, this type of approach defines a value for the percentage of pixels in the images, or *p-tile*, probably belonging to fiber segment edges, of higher gradient magnitude. This approach, which is also known as the *p-tile* method, does not assures the selection of the optimum threshold for each image, being quite sensitive to variations in the level of noise introduced into the image (e.g., promoted by small variations in the level of illumination) [40]. To avoid these problems, the GSM algorithm developed in this work included the application of an automatic segmentation method to determine the optimum threshold for each image, the Otsu's method [40,49]. The two sets of pixels (i.e., fiber segment edges and background) contribute with distinct distributions to the histogram of gradient magnitudes (180 bins were considered) [40]. Therefore, the Otsu's method tests all possible thresholds, allowing the optimum value maximizing the separation between the two sets of pixels to be obtained [49].

2.3.3. Obtaining the frequency distribution for the angles of fiber segments

In the proposed GSM (gradient-segmentation method) approach, the pixels determined as being part of a fiber segment edge (i.e., pixels with gradient magnitude values above the threshold) are assumed to have equal contribution to the frequency distribution for the angles of fiber segments (−180° to 180°), which is also known as the frequency distribution of fiber segments orientation, being assigned to the corresponding bin (i.e., range of angles). This approach contrasts with the

procedure previously developed by Erkkilä and co-authors [31,45,46], in which all pixels of the image contribute to the frequency distribution by using the gradient magnitude as the weighting factor. This approach, designated in this work as the weighted gradient method or WGM, was also compared to the proposed GSM method. It should be mentioned that Erkkilä and co-authors used the WGM method combined with convolution masks of higher complexity (5 × 5 matrices) to estimate the gradient of intensities [45]. In this work, the two approaches, GSM and WGM, were both combined with simpler convolution masks of the Sobel operator. A preliminary study indicated that the number of bins of the frequency distribution of fiber orientation does not have a statistically significant effect on the results (see Fig. A.1 in Appendix A). The number of bins was then set to 105, corresponding to a range of angles of around 3.4° per bin.

2.3.4. Fitting a fiber orientation model to the frequency distribution data

The data of the frequency distribution of fiber segments orientation are fitted by a Fourier series expansion truncated in the third term, $f_\theta(\theta)$, designated in this work as the cosine function with three terms, Eq. (5) [50,51]:

$$f_\theta(\theta) = \frac{K}{\pi}(1 + \eta_1 \cos(2(\theta - \theta_{max})) + \eta_2 \cos(4(\theta - \theta_{max})) + \eta_3 \cos(6(\theta - \theta_{max}))) \quad (5)$$

Where, K is a scale factor, θ_{max} is the orientation angle, corresponding to the angle at the maximum of the function, and η_1, η_2 and η_3 are the three terms considered of the truncated Fourier series expansion. The anisotropy A of the fiber orientation distribution is then obtained by the ratio maximum/minimum of the fitted function.

2.4. Internal and external validation of the proposed in-plane fiber orientation measurement system

The proposed methodology was assessed both by analyzing its internal consistency with imposed sheet rotations (internal validation) and by comparison against a reference method (external validation). The internal validation was performed for the sample surface with higher anisotropy value, while the external validation was conducted for all samples.

The internal consistency assessment consists in analyzing if the change in fiber orientation provided by the proposed methodology, for a paper sheet that was rotated with a known offset angle (θ_{off}), accurately match the rotation angle. To pass the internal validation test, a 1:1 relationship should exist between the estimated orientation angle (θ_{max}) and the offset angle (θ_{off}), while providing approximately constant values for the anisotropy (A). In this work, two types of indicators were used to determine the level of internal consistency of the image analysis based method: i) the coefficient of determination, R^2, of the linear regression of the orientation angle as a function of the offset angle, $\theta_{max} = r_1 \times \theta_{off} + r_2$; ii) the average value of the modulus of relative deviation, $\overline{|\boldsymbol{RD}|}$, of the anisotropy values at a given offset angle point i, A_i, from the standard measurement ($\theta_{off} = 0°$), $A(0°)$, determined by Eq. (6):

$$\overline{|RD|} = \sum_{i=1}^{n=6} \frac{|RD|_i}{n} \quad (6)$$

where $|RD|_i$ is the absolute value of the relative deviation of the anisotropy at a given offset angle with index i, expressed as a percentage, Eq. (7), and n is the number of rotations tested.

$$|RD|_i = \frac{|A_i - A(0°)|}{A(0°)} \times 100\% \quad (7)$$

The results of $\overline{|\boldsymbol{RD}|}$ are presented together with the corresponding standard errors, $\overline{|\boldsymbol{RD}|} \pm \sigma_{avg}$, where σ_{avg} is the standard deviation of the mean (also known as the standard error of the mean), estimated from the sample standard deviation of the n data points, $\hat{\sigma}$, using the formula in Eq. (8):

$$\sigma_{avg} = \frac{\hat{\sigma}}{\sqrt{n}} \quad (8)$$

As mentioned before, the small area of the images obtained with the camera motivated the use of 8 images per sample surface to obtain averages of the anisotropy and of the orientation angle. These results were also used to confirm the statistical significance of the differences observed in different samples, during the validation stage through a two-sample student's t-test (significance level of 0.05).

The external validation was accomplished comparing the measurements provided for the three paper samples by the proposed system against those from a reference method widely used in the industry, the ultrasonic based TSO technique [23,24]. The TSO technique measures the tensile stiffness orientation distribution, a property highly correlated with the fiber orientation [11,18–20]. However, TSO measurements are also dependent on the drying conditions [13,20,24], a fact that was also taken into account when performing the comparison with the developed image analysis approach. It should also be mentioned that the three paper samples are used only for independent testing purposes. In other words, they represent distinct testing scenarios, were the methods should operate accurately. In particular, the papers have different anisotropy levels.

In the next section, the results obtained during the development and validation stages of the proposed methodology are presented in detail.

3. Results and discussion

The methodology developed in this work combines the image analysis algorithm GSM with an imaging system based on a digital camera, being appropriately designated as the camera-GSM approach. In this section, an overview of the methodology is initially shown. Subsequently, the internal and external validation studies are presented and discussed.

3.1. Overview of the proposed methodology

To provide a general idea of the different steps of the proposed methodology, a sequence of snapshots of the entire protocol is presented next. In Fig. 4 it is possible to observe images obtained with the camera based imaging system for the laboratory paper sample S3, in the bottom and top surfaces. The imaging system was developed to acquire images with improved quality. An apparatus based on image analysis has been previously proposed in the literature, consisting of a digital camera combined with an illumination system formed by light sources in a ring like disposition. The emitted light is directed to the paper surface, forming relatively high angles of 30° to 75° [32]. A similar concept, but with a distinct light arrangement was developed in this work. In our system, a digital camera is coupled to a low angle illumination system based on a ring of LEDs, with the emitted light forming an angle with the paper surface which is inferior to 30°, in order to enhance the contrast between fibers.

As mentioned before, the protocol we have followed to prepare the laboratory sheets promoted rougher top surfaces when compared to the bottom surfaces. This fact was confirmed by roughness measurements with a Bendtsen tester: higher roughness values of around 470 ml/min were obtained for the top surfaces of the samples, contrasting to the lower values of around 190 ml/min for the bottom surfaces. The use of a low angle illumination system improved the quality of the obtained images, with the contrast between fibers being increased due to the reduction of the reflected light from highly reflecting regions [30]. This greatly improves image quality and allows to visually perceive the difference in roughness between the top and bottom surfaces (see Fig. 4). Most importantly, the improved imaging system enables the successful use of gradient based algorithms, such as the new GSM method, to

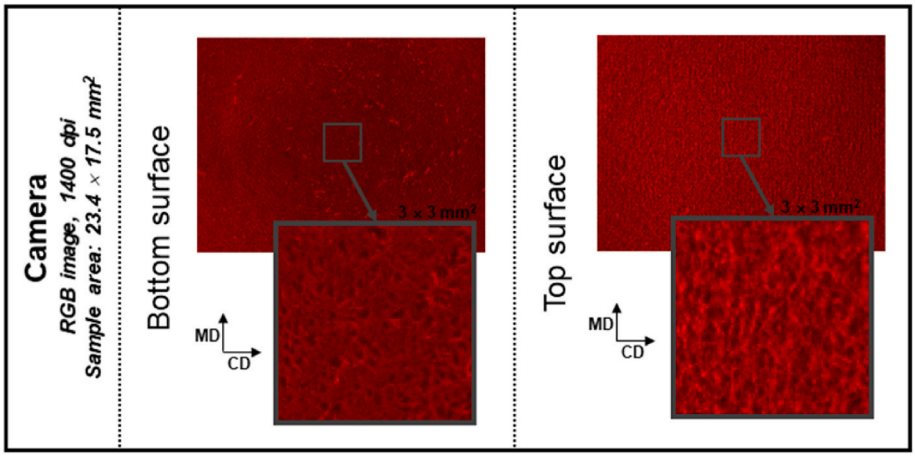

Fig. 4. Images obtained for the two surfaces of sample S3, bottom and top, with a digital camera coupled to a low angle illumination system.

analyze paper surfaces [32]. Typically, the gradient based algorithms found in the literature have been used to analyze reflective based images of paper layers obtained by sheet splitting [5,6,31,41,45,46]. Higher contrast between fibers are inherently promoted by the application of a sheet splitting technique to the paper sheets, allowing the determination of the fiber orientation distribution of the obtained layers from reflective based images of lower quality (resolution of only 600 to 800 dpi).

The application of the gradient based GSM algorithm to an image of the top surface of sample S3 is presented in Fig. 5, including the histogram of gradient magnitudes, in which the threshold is obtained by the Otsu's method to define the pixels of fiber segment edges, and the relative frequency data of fiber orientation, represented in a polar coordinate system and fitted by the cosine function with three terms. The small digitalized sample area combined with the relatively low camera resolution of 1400 dpi leads to fiber orientation distribution with some degree of unevenness, in line with previous studies in the literature [45].

The GSM algorithm makes use of a lower number of pixels, avoiding the contribution of pixels that are probably not part of a fiber segment edge. Additionally, the use of an adaptive scheme based on the Otsu's method assures the selection of an optimum threshold for each image, in contrast to the ad hoc selection of a constant value to apply to all the images implemented by the *p-tile* thresholding method [40]. This makes the GSM approach more robust to image and illumination artifacts. In practice, the GSM algorithm determines the percentage of pixels considered as being part of fiber segment edges (also known as *p-tile*), allowing a direct comparison with the *p-tile* thresholding method. Fig. 6 presents the evolution of the orientation angle and of the anisotropy

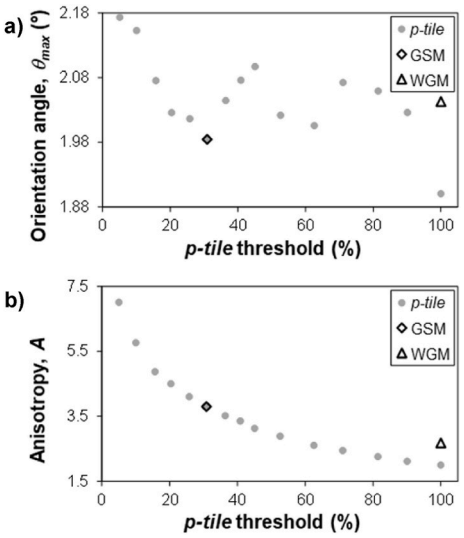

Fig. 6. Comparison of the GSM and WGM algorithms with the application of the *p-tile* method for several thresholds to analyze an image of sample surface S3T obtained by a digital camera with low angle illumination: a) orientation angle, θ_{max}; b) anisotropy, A.

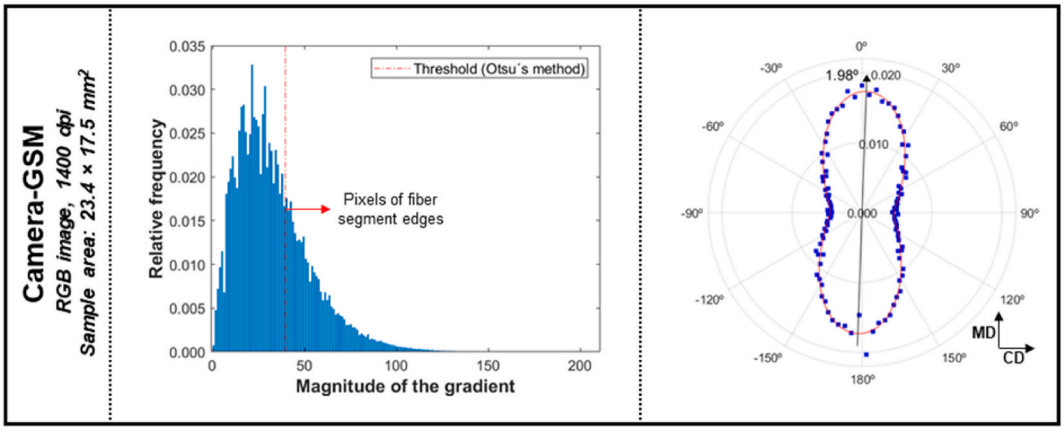

Fig. 5. Application of the gradient-segmentation method (GSM) to an image of sample surface S3T obtained by a digital camera with low angle illumination (camera-GSM): histogram of gradient magnitudes (left column) and corresponding fiber orientation distribution (right column).

with different *p-tile* thresholds for an image of sample S3T. The results of the GSM algorithm are shown for the corresponding *p-tile* value. The results obtained with the WGM method are also shown. In contrast to the thresholding methods, the WGM algorithm considers the contribution of all the pixels weighed by the gradient magnitude [45,46].

The orientation angle is not affected by the selected threshold, being kept reasonably constant and similar to the one obtained by the WGM method. On the other hand, the anisotropy varies with the applied threshold, confirming the importance of using an adaptive thresholding scheme to avoid the negative effect of possible image and illumination artifacts, as implemented in the GSM algorithm. Additionally, the anisotropy value obtained by the WGM method was slightly inferior to the one obtained by the GSM algorithm. A more comprehensive comparison between the GSM and WGM algorithms can be seen in Section 3.3.

3.2. Internal validation

The internal consistency is assessed by rotating a sample surface with a known offset angle (θ_{off}) relative to MD at the imaging step. Preliminary results (not shown in this work) obtained for a imaging apparatus with a non-symmetrical illumination system indicated that samples with higher anisotropy values are more likely to present measurement issues due to shadow illumination effects, in particular for the cases where the fiber orientation angle is clearly misaligned with MD ($\theta_{max} > 15°$). Therefore, the offset study was conducted for the sample surface S3T, with higher anisotropy. The results obtained for the developed camera-GSM methodology are shown in Fig. 7. Error bars were added to the data points, corresponding to the standard deviation.

A near linear relationship between the orientation angle and the offset angle was observed, with an R^2 of 0.9975 being obtained. Additionally, a reduced variation of the anisotropy with the offset angle was detected, producing a low $\overline{|RD|}$ of 13.1% ± 2.8%. Most importantly, the anisotropy was kept virtually constant till an offset angle of 15°, within the range of angles that are probably present at the paper machine under normal operational conditions [52,53]. These results indicate the high internal consistency level of the developed methodology, confirming the potential of combining a digital camera with a low angle illumination system for the quantitative analysis of fiber orientation at the paper surface. The results are even more interesting considering the relatively low resolution of 1400 dpi of the camera used in this work, suggesting that even better results could probably be obtained by using a digital camera with higher resolution.

3.3. External validation

Fig. 8 presents the results of fiber orientation distribution parameters (orientation angle and anisotropy) obtained for the 3 sheets by the developed camera-GSM methodology and by the reference method TSO, an ultrasonic based technique. In addition, the results obtained by the camera-WGM configuration are also shown. As expected, this configuration combines the developed camera based imaging system with the WGM algorithm proposed in the literature [31,45,46]. Error bars were added to the data points of the camera based approaches, corresponding to the standard deviation.

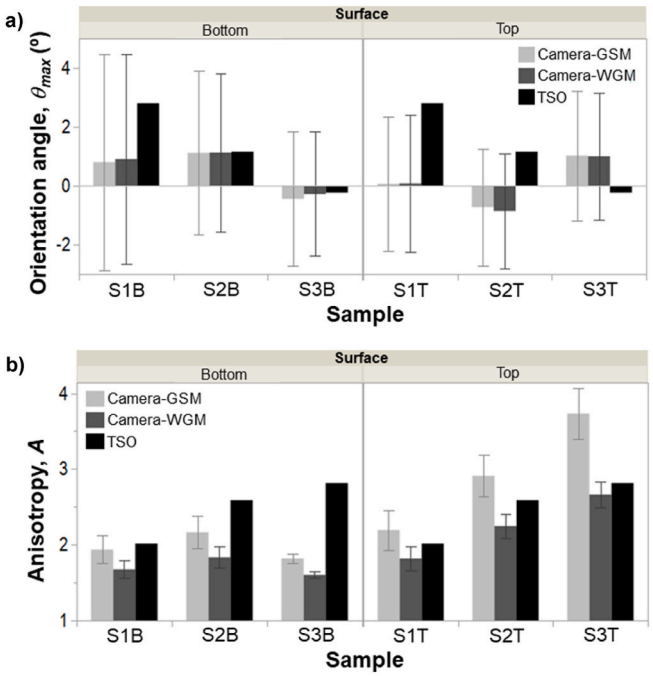

Fig. 8. Comparison of fiber orientation determined by the developed camera based imaging method (RGB, 1400 dpi, 23.4 × 17.5 mm^2) coupled to two different algorithmic approaches, GSM and WGM, and by TSO, used as reference, for the studied samples S1, S2 and S3: a) orientation angle, θ_{max}; b) anisotropy, *A*.

First, the two image analysis algorithms, GSM and WGM, were compared. The algorithms presented identical values of the orientation angle for the analyzed samples, as seen in Fig. 8. The algorithms also provided similar tendencies for the anisotropy of the three sheets, with slightly higher values being obtained by the GSM method. These results confirmed the GSM method to be a reliable alternative to the WGM algorithm. As such, the corresponding camera-GSM methodology was subsequently compared with the reference TSO method, for validation. The TSO method determines the TSI (tensile stiffness index) orientation distribution, being highly dependent on the applied drying restraints

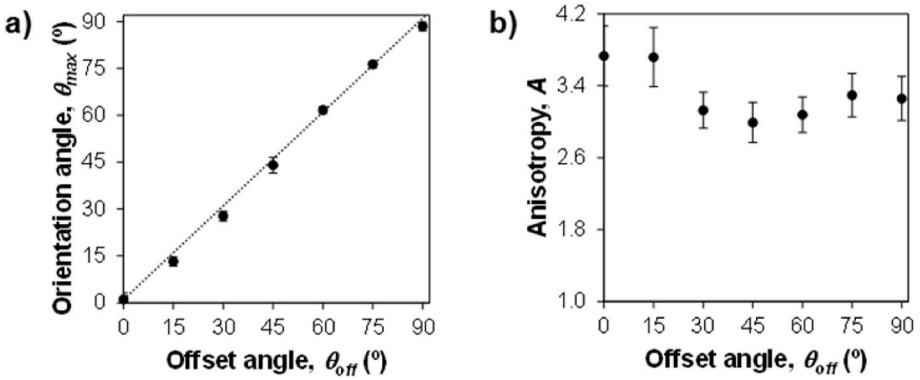

Fig. 7. Assessment of the internal consistency of the camera-GSM methodology (RGB, 1400 dpi, 23.4 × 17.5 mm^2), by analyzing the effect of introduced offset angles, θ_{off}, to the sample surface S3T on the measurement of: a) orientation angle, θ_{max}; b) anisotropy, *A*.

[12,13,19–21,24]. However, for sheets dried under biaxial restraint (i.e., restraint applied in CD and in MD), similar to the conditions used in this work, the TSO results correlate well with the fiber orientation distribution [13,54,55].

As expected, the TSO technique detected the different anisotropy levels of the analyzed samples. This result was confirmed by the camera-GSM methodology for the top surfaces. In particular, the *t*-Test was applied to the three pairs of samples (S1T/S2T, S1T/S3T and S2T/S3T), with statistically significant differences being found between the anisotropy averages (p-values of 0.0001). Additionally, the results of the orientation angle obtained by the camera-GSM approach for the top surfaces were similar to the values determined by the TSO measurements. On the other hand, the camera-GSM approach could not distinguish correctly between the different anisotropy levels of the bottom surfaces, with similar values being obtained for the three samples. As mentioned previously, the bottom-surface samples are smoother (see Fig. 4), most probably requiring a camera with a higher resolution than 1400 dpi to correctly isolate fibers in the bottom surfaces. Previous studies have also shown that the fiber anisotropy near the surface might not always correlate with the overall fiber orientation of the sample [31,56,57], which could explain, at least partially, the results observed for the bottom surfaces. Nevertheless, the orientation angles obtained for the bottom surfaces were similar to the values measured with TSO. Therefore, future work should focus on testing a higher resolution digital camera with the low angle illumination system, which should in principle increase the already high internal consistency level of the method while improving at the same time the capacity to analyze images of smoother sheets such as those of the bottom surface of the studied samples.

The growing trend of digitalization in Industry 4.0 favors the development of online measurement systems to monitor in real time important process variables [47]. The proposed GSM algorithm requires less than 3 seconds to analyze an image of a paper sample (regular laptop used). In this context, the developed camera-GSM approach has the potential for harnessing quality online measurements in the paper machine under real industrial operating conditions, in particular for the cases were edge computing is implemented. As such, the camera-GSM approach is an interesting alternative to previously proposed methodologies found in the literature [27,32].

4. Conclusions

A fast, portable and inexpensive methodology to estimate the in-plane fiber orientation at the surface of laboratory paper sheets was successfully developed and implemented. It combines a reflective imaging method based on a digital camera, to obtain images of paper surfaces, with the new and robust image processing algorithm GSM, to determine the polar fiber orientation distribution, being appropriately designated as the camera-GSM methodology. The digital camera was combined to a low angle illumination system, to improve the quality of the acquired images. The proposed GSM algorithm makes use of a lower number of pixels due to the implementation of an adaptive thresholding scheme, avoiding the contribution of pixels that are probably not part of a fiber segment edge. This adaptive scheme also assures the selection of an optimum threshold for each image, in contrast to the ad hoc selection of a constant value to apply to all the images.

The camera-GSM methodology presented a high internal consistency, accurately identifying introduced offset angles relative to MD at the imaging step. Additionally, the methodology successfully distinguished sheets of different anisotropy levels by analyzing the rougher top surfaces. However, the methodology could not effectively distinguish the different anisotropy levels for the smoother bottom sample surfaces. It is known that the fiber orientation in the surface might not always correlate with the distribution of the overall sample. Nevertheless, the camera low resolution of 1400 dpi could have also contributed to some extent to this result. As such, the use of a higher resolution camera should potentially improve the capability to analyze sheets with smoother surfaces. Moreover, the camera solution offers the capability for online measurements, opening the possibility for an industrial application of the developed methodology in the paper machine, promoting the digitalization efforts of Industry 4.0. Therefore, future work will focus on the optimization of the proposed camera-GSM method (e.g., higher resolution camera) and in the subsequent steps to transfer it to the process.

Author statement

Paulo A.N. Dias: Conceptualization, Methodology, Software, Investigation, Writing – original draft, Writing – review & editing. Ricardo Jorge Rodrigues: Supervision, Resources. Marco S. Reis: Conceptualization, Methodology, Writing – review & editing, Supervision, Resources.

Declaration of competing interest

The authors declare that they have no known competing financial interests or personal relationships that could have appeared to influence the work reported in this paper.

Data availability

The data that has been used is confidential.

Acknowledgments

This work was carried out under the Project inpactus – innovative products and technologies from eucalyptus, Project N.º 21874 funded by Portugal 2020 through European Regional Development Fund (ERDF) in the frame of COMPETE 2020 nº246/AXIS II/2017. Marco S. Reis acknowledges support from the Chemical Process Engineering and Forest Products Research Center (CIEPQPF), which is financed by national funds from FCT/MCTES (reference UID/EQU/00102/2020).

Appendix A. Effect of the number of bins used in the frequency distribution of fiber orientation

A preliminary analysis was conducted to assess the effect of the number of bins used in the frequency distribution of fiber orientation, regarding the determination of the parameters of interest, anisotropy (A) and orientation angle (θ_{max}). The study was performed to an image of the top surface of sample S3 obtained by the developed camera-based imaging system. The fiber orientation was determined by the new GSM algorithm and by the WGM method found in the literature. The results indicated that the number of bins used does not have a statistically significant impact on the values obtained of the fiber orientation parameters (see Fig. A.1). Therefore, the number of bins was set to 105.

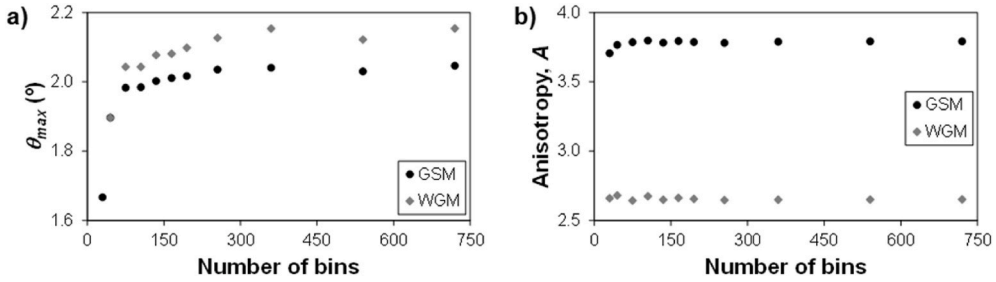

Fig A1. Effect of the number of bins of the histogram of fiber orientation distribution (−180° to 180°) of an image acquired with a camera with a low angle illumination system (RGB, 1400 dpi, 23.4 × 17.5 mm^2) of sample surface S3T on properties calculated by applying two image analysis approaches, GSM and WGM: a) orientation angle, θ_{max}; b) anisotropy, A.

References

[1] D.H. Page, The beating of chemical pulps - the action and the effects, in: C.F. Baker (Ed.), Fundamentals of Papermaking - Transactions of the 9th Fundamental Research SymposiumCambridge, 1989, pp. 1–38. UK.

[2] D.H. Page, R.S. Seth, B.D. Jordan, M.C. Barbe, Crimps Curl, Kinks and Microcompressions in Pulp Fibres - Their Origin, Measurement and Significance, Transactions of the 8th Fundamental Research SymposiumOxford, UK, 1985, pp. 183–227.

[3] T. Enomae, Y. Han, A. Isogai, Nondestructive determination of fiber orientation distribution of paper surface by image analysis, Nord. Pulp Pap Res. J. 21 (2006) 253.

[4] A.d.O. Mendes, P.T. Fiadeiro, A.P. Costa, M.E. Amaral, M.N. Belgacem, Laser scanning for assessment of the fiber anisotropy and orientation in the surfaces and bulk of the paper, Nord. Pulp Pap Res. J. 30 (2015) 308–318.

[5] M.D. Lloyd, I.R. Chalmers, Use of an Image Orientation Analysis Technique to Investigate Sheet Structural Problems during Forming, 54th Appita Annual ConferenceMelbourne, Australia, 2000, pp. 495–502.

[6] M.D. Lloyd, I.R. Chalmers, Use of fibre orientation analysis to investigate sheet structural problems during forming, Appita J. 54 (2001) 15–21.

[7] C. Fellers, The structure of paper and its modelling, in: M. Ek, G. Gellerstedt, G. Henriksson (Eds.), Paper Products Physics and Technology, Walter de Gruyter GmbH & Co., Berlin, Germany, 2009, pp. 1–24.

[8] T. Wahlstrom, Predictions of MD and CD Tensile Property Profiles, 15th Fundamental Research SymposiumCambridge, UK, 2013, pp. 673–710.

[9] J.T. Decker, A.A. Khaja, M.T. Hoang, J.M. Considine, D.W. Vahey, K.T. Turner, R. E. Rowlands, Variation of paper curl due to fiber orientation, in: T. Proulx (Ed.), Society for Experimental Mechanics Annual Conference, Springer, New York, Indianapolis, Indiana, US, 2010, pp. 347–352.

[10] A.-L. Erkkila, T. Leppanen, A. Puurtinen, M. Ora, T. Tuovinen, Hygroexpansivity of anisotropic sheets, Nord. Pulp Pap Res. J. 30 (2015) 326–335.

[11] K.J. Niskanen, J.W. Sadowski, Evaluation of some fibre orientation measurements, J. Pulp Pap. Sci. 15 (1989) J220–J224.

[12] M. Titus, Ultrasonic technology: measurements of paper orientation and elastic properties, Tappi J. 77 (1994) 127–130.

[13] T.R. Hess, P.H. Brodeur, Effects of wet straining and drying on fibre orientation and elastic stiffness orientation, J. Pulp Pap. Sci. 22 (1996) J160–J164.

[14] U. Hirn, W. Bauer, Evaluating an Improved Method to Determine Layered Fibre Orientation by Sheet Splitting, 61st Appita Annual Conference and ExhibitionGold Coast, Australia, 2007, pp. 71–79.

[15] U. Hirn, W. Bauer, Investigating Paper Curl by Sheet Splitting, EUCEPA Conference `Challenges 06, Bratislava, Slovakia, 2006.

[16] J. Scharcanski, C.T.J. Dodson, Texture image analysis for paper anisotropy and its variability, Appita J. 49 (1996) 100–104.

[17] G.A. Baum, C.C. Habeyer, The use of microwave attenuation as a measure of fiber orientation anisotropy, Tappi J. 70 (1987) 109–113.

[18] H.J. Schaffrath, O. Tillmann, Testing of fibers, suspensions, and paper and board grades, in: H. Holik (Ed.), Handbook of Paper and Board, Wiley-VCH Verlag GmbH & Co. KGaA, Weinheim, Germany, 2013, pp. 1059–1086.

[19] Z. Tan, Paper: nondestructive evaluation, in: K.H.J. Buschow, R.W. Cahn, M. C. Flemings, B. Ilschner, E.J. Kramer, S. Mahajan, P. Veyssiere (Eds.), Encyclopedia of Materials: Science and Technology, Elsevier, Oxford, 2001, pp. 1–5.

[20] P. Brodeur, J.P. Gerhardstein, Overview of Applications of Ultrasonics in the Pulp and Paper Industry, 1998, IEEE Ultrasonics SymposiumSendai, Japan, 1998, pp. 809–815.

[21] G.A. Baum, Polar Diagrams of Elastic Stiffness: Effect of Machine Variables, 1987 International Paper Physics ConferenceAuberge Mont Gabriel, 1987, pp. 161–166. Quebec, Canada.

[22] J.F. Waterhouse, Ultrasonic testing of paper and paperboard: principles and applications, Tappi J. 77 (1994) 120–126.

[23] D.W. Vahey, J.M. Considine, Surface and Subsurface Fiber-Orientation-Angle Measurements in Three Office Papers, PaperCon 2008 TAPPI/PIMA Paper Conference and Trade Show, TAPPI Press, Dallas, Texas, USA, 2008, pp. 1–9.

[24] D.W. Vahey, J.M. Considine, A. Kahra, M. Scotch, Progress in Paper Physics Seminar 2008Espoo, in: Comparison of Fiber Orientation and Tensile-Stiffness Orientation Measurements in Paper, Finland, 2008, pp. 271–273.

[25] C.F. Yang, C.M. Crosby, A.R.K. Eusufzai, R.E. Mark, Determination of paper sheet fiber orientation distributions by a laser optical diffraction method, J. Appl. Polym. Sci. 34 (1987) 1145–1157.

[26] K.J. Niskanen, J.W. Sadowski, Fiber orientation in paper by light diffraction, J. Appl. Polym. Sci. 39 (1990) 483–486.

[27] A.A. Hellstrom, W.A. Gregory, Method and Apparatus for On-Line Determination of Fiber Orientation and Anisotropy in a Non-woven Web, ABB Industrial Systems, Inc., 1997.

[28] A.d.O. Mendes, P.T. Fiadeiro, A.P. Costa, M.E. Amaral, M.N. Belgacem, in: M.F.P.C. M. Costa (Ed.), Retro-diffusion and Transmission of Laser Radiation to Characterize the Paper Fiber Distribution and Mass Density, 8th Iberoamerican Optics Meeting and 11th Latin American Meeting on Optics, Lasers, and Applications, International Society for Optics and Photonics, Porto, Portugal, 2013, p. 8785AY.

[29] T. Enomae, Y.-H. Han, A. Isogai, Z-directional distribution of fiber orientation of Japanese and western papers determined by confocal laser scanning microscopy, J. Wood Sci. 54 (2008) 300–307.

[30] T. Enomae, Y.-H. Han, A. Isogai, Fiber Orientation Distribution of Paper Surface Calculated by Image Analysis, International Papermaking and Environment Conference 2004Tianjin, P. R. China, 2004, pp. 355–368.

[31] A.-L. Erkkila, P. Pakarinen, M. Odell, Sheet forming studies using layered orientation analysis, Pulp and Paper Canada 99 (1998) 81–85.

[32] J.F. Shakespeare, M.M. Kellomaki, Method and Apparatus for Measuring Fiber Orientation of a Moving Web, Honeywell International Inc., 2006.

[33] P. Facco, E. Tomba, M. Roso, M. Modesti, F. Bezzo, M. Barolo, Automatic characterization of nanofiber assemblies by image texture analysis, Chemometr. Intell. Lab. Syst. 103 (2010) 66–75.

[34] P. Facco, A.C. Santomaso, M. Barolo, Artificial vision system for particle size characterization from bulk materials, Chem. Eng. Sci. 164 (2017) 246–257.

[35] G. Chinga-Carrasco, Exploring the multi-scale structure of printing paper-a review of modern technology, J. Microsc. 234 (2009) 211–242.

[36] M.S. Reis, A. Bauer, Wavelet texture analysis of on-line acquired images for paper formation assessment and monitoring, Chemometr. Intell. Lab. Syst. 95 (2009) 129–137.

[37] S. Kärkkäinen, E.B.V. Jensen, Estimation of fibre orientation from digital images, Image Anal. Stereol. 20 (2001) 199–202.

[38] L. Xu, I. Parker, Y. Filonenko, A New Technique for Determining Fibre Orientation Distribution through Paper, 1999 International Paper Physics Conference, 1999, pp. 421–427. TAPPI, San Diego, USA.

[39] J.L. Thorpe, Exploring Fibre Orientation within Copy Paper, 1999, International Paper Physics ConferenceSan Diego, USA, 1999, pp. 447–458.

[40] M. Sonka, V. Hlavac, R. Boyle, Image Processing, Analysis, and Machine Vision, fourth ed., Cengage Learning, Stamford, USA, 2014.

[41] F. Rosen, D. Soderberg, M.F. Lucisano, C. Östlund, Estimation of Fibre Segment Orientation Using Steerable Filtering, PaperCon'08 - Paper Conference and Trade Show, TAPPI Press, Dallas, TX, United States, 2008, pp. 1097–1144.

[42] J. Scharcanski, C.T.J. Dodson, Local spatial anisotropy and its variability, J. Pulp Pap. Sci. 25 (1999) 393–397.

[43] J. Scharcanski, C.T.J. Dodson, Texture analysis for estimating spatial variability and anisotropy in planar stochastic structures, Opt. Eng. 35 (1996) 2302–2309.

[44] J. Scharcanski, C.T.J. Dodson, Stochastic texture image estimators for local spatial anisotropy and its variability, IEEE Trans. Instrum. Meas. 49 (2000) 971–979.

[45] P. Lipponen, A.-L. Erkkilä, T. Leppänen, J. Hämäläinen, On the Importance of In-Plane Shrinkage and Through-Thickness Moisture Gradient during Drying on Cockling and Curling Phenomena, 14th Pulp and Paper Fundamental Research SymposiumOxford, UK, 2009, pp. 389–436.

[46] A.-L. Erkkilä, T. Leppänen, T. Tuovinen, The curl and fluting of paper : the effect of elasto-plasticity, in: M. Papadrakakis, V. Papadopoulos, G. Stefanou, V. Plevris (Eds.), ECCOMAS Congress 2016 : VII European Congress on Computational Methods in Applied Sciences and EngineeringCrete, 2016, pp. 4752–4769. Greece.

[47] M.S. Reis, G. Gins, Industrial process monitoring in the big data/industry 4.0 era: from detection, to diagnosis, to prognosis, Processes 5 (2017) 35.

[48] D. Neiva, L. Fernandes, S. Araújo, A. Lourenço, J. Gominho, R. Simões, H. Pereira, Chemical composition and kraft pulping potential of 12 eucalypt species, Ind. Crop. Prod. 66 (2015) 89–95.
[49] N. Otsu, A threshold selection method from gray-level histograms, IEEE Trans.Sys., Man, Cyber. 9 (1979) 62–66.
[50] R.W. Perkins Jr., Models for describing the elastic, viscoelastic, and inelastic mechanical behaviour of paper and board, in: R.E. Mark, C.C. Habeger Jr., J. Borsch, M.B. Lyne (Eds.), Handbook of Physical Testing of Paper, Marcel Dekker, New York, USA, 2002, pp. 1–75.
[51] T. Wahlström, Prediction of Fibre Orientation and Stiffness Distributions in Paper–An Engineering Approach, 14th Fundamental Research SymposiumOxford, UK, 2009, pp. 1039–1078.
[52] M.H. Odell, P. Pakarinen, The Compleat Fibre Orientation Control and Effects on Diverse Paper Properties, 2001 Papermakers ConferenceAtlanta, 2001. Georgia, USA.
[53] A. Hellstrom, The Two Sides of Fiber Orientation, 2005 TAPPI Practical Papermaking ConferenceMilwaukee, Wisconsin, USA, 2005.
[54] T. Wahlstrom, The Invariant Shrinkage and Stiffness of Paper–Modeling Anisotropic Behaviour Based on Isotropic Handsheets, the 2004 Progress in Paper Physics SeminarTrondheim, 2004, pp. 105–108. Norway.
[55] T. Wahlstrom, P. Mäkelä, Predictions of Anisotropic Multiply Board Properties Based on Isotropic Ply Properties and Drying Restraints, 13th Fundamental Research SymposiumCambridge, UK, 2005, pp. 241–281.
[56] U.M. Haggblom-Ahnger, P.I. Pakarinen, M.H. Odell, D.E. Eklund, Conventional and stratified forming of office paper grades, Tappi J. 81 (1998) 149–158.
[57] M.H. Odell, Paper structure engineering, Appita J. 53 (2000) 371–377.